


Cite this: *RSC Adv.*, 2025, **15**, 35913

Received 30th July 2025
Accepted 21st September 2025

DOI: 10.1039/d5ra05514h

rsc.li/rsc-advances

Synthesis and antitumor activity of steroid-based imidazolium salts

Tingting Li, Yu Pan, Yuanyuan Peng, Aoran Li, Moyi Huang, Leijie Fu, Yongli Li, Zihan Zhang, Lingmei Kong* and Guogang Deng *

A total of thirty-six novel diosgenin-, cholesterol-, and dehydroepiandrosterone-imidazolium salt derivatives were synthesized and their cytotoxic activities were evaluated *in vitro* against a panel of human tumor cell lines. The SAR results indicated that the presence of a substituted 5,6-dimethylbenzimidazole ring and the substitution at the imidazolyl-3-position with a 1-naphthylmethyl or 4-methylbenzyl group could be critical for enhancing cytotoxic activity. Dehydroepiandrosterone-imidazolium salt **12f** was found to be the most potent compound with IC_{50} values of 1.07–2.10 μM against MDA-MB-231, HepG2 and 22RV1 human tumor cell lines. Furthermore, cell cycle and apoptosis experiments of compound **12f** were carried out and the results showed that **12f** could induce G0/G1 cell cycle arrest and apoptosis in HepG2-116 cells.

Introduction

Cancer ranks as the second leading cause of death globally.¹ It was estimated that there were approximately 20 million new cancer cases alongside 9.7 million deaths due to cancer in 2022, and the number of new cancer cases will reach 35 million by 2050.² Drug therapy remains the primary clinical antitumor treatment for many patients up to this day. Natural products have held a pivotal position in drug discovery, serving as the foundation for the majority of early medicinal formulations.³ A comprehensive analysis of all new molecular entities approved by the FDA has shown that natural products and their derivatives comprise more than one-third of these newly approved molecular entities.⁴

Steroids play a pivotal role in drug discovery and have been referred to as the “keys to life” by Rupert Witzmann. These molecules possess a wide range of biological activities, including antitumor,⁵ anti-inflammatory,⁶ anti-bacterial⁷ and immunomodulatory⁸ effects. Steroid-based drugs exhibit a wide range of clinical therapeutic applications and remain among the top-selling categories of pharmaceuticals on the market.⁹

On the other hand, imidazolium salts have attracted considerable attention in the research community owing to their diverse biological and pharmacological activities,¹⁰ particularly their prominent antitumor properties.¹¹ Given the circumstances, our group has been committed to the synthesis of novel imidazolium salt derivatives and successfully identified

a series of promising compounds that exhibit significant antitumor activity.¹² For example, compound **60** (Fig. 1) demonstrated significant inhibitory effects on MCF-7 tumor cells with IC_{50} values of 1.04 μM , approximately tenfold lower than cisplatin ($IC_{50} = 10.64 \mu\text{M}$).¹³ Compound **a6** (Fig. 1) demonstrated potent cytotoxic activity against HepG2, A-549, MDA-MB-231 and HCT-116 with IC_{50} values of 0.04–0.29 μM .¹⁴ Mechanism studies have shown that the steroid imidazolium salt **a30** (Fig. 1) and other imidazolium salts can inhibit cell proliferation by inducing cell cycle arrest and apoptosis.¹⁵ Moreover, **B591** (Fig. 1) has been proven to be a novel pan-PI3K inhibitor, which can effectively inhibit class I PI3K isoforms, blocking the PI3K/mTOR pathway.¹⁶

In recent decades, the progress of drug discovery has become increasingly linked to advancements in synthetic organic chemistry.¹⁷ It is worth noting that the urgent need to rapidly

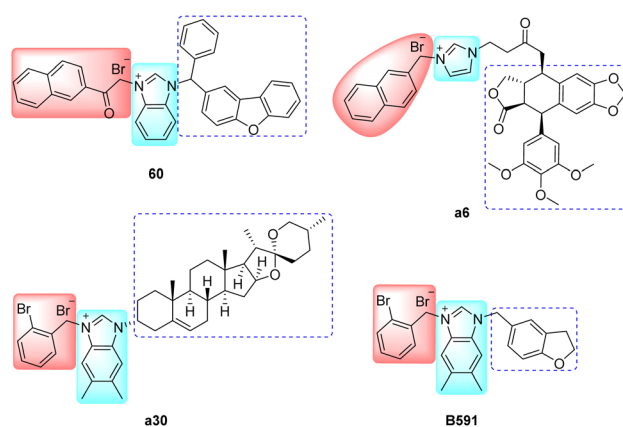


Fig. 1 Representative structures of imidazolium salts.



diversify existing lead structures for structure–activity relationship (SAR) studies has further emphasized the critical importance of designing efficient, modular, and expedited synthetic protocols.¹⁸ The synergy between drug discovery and chemical synthesis can accelerate the optimization of drug molecule properties.

In this context, we investigated the SAR of imidazolium salt derivatives^{15a} that were previously obtained by modifying steroid compounds using molecular hybridization. Our findings indicate that the presence of 5,6-dimethylbenzimidazole ring and substitution at the 3-position of the imidazole ring with groups such as 2-bromobenzyl or 2-naphthyl are critical for antitumor activity. These insights provide critical guidance for the rational design and synthesis of imidazolium salts, facilitating the development of more effective antitumor agents. Furthermore, to the best of our knowledge, no studies have reported the synthesis of steroidal imidazolium salt derivatives by extending the carbon chain between the steroid skeleton and the imidazole ring using linking subunits. Based on these considerations, we systematically investigated the synthesis and antitumor activity of a series of novel steroidal imidazolium salt derivatives and present our findings herein.

Results and discussion

Chemistry

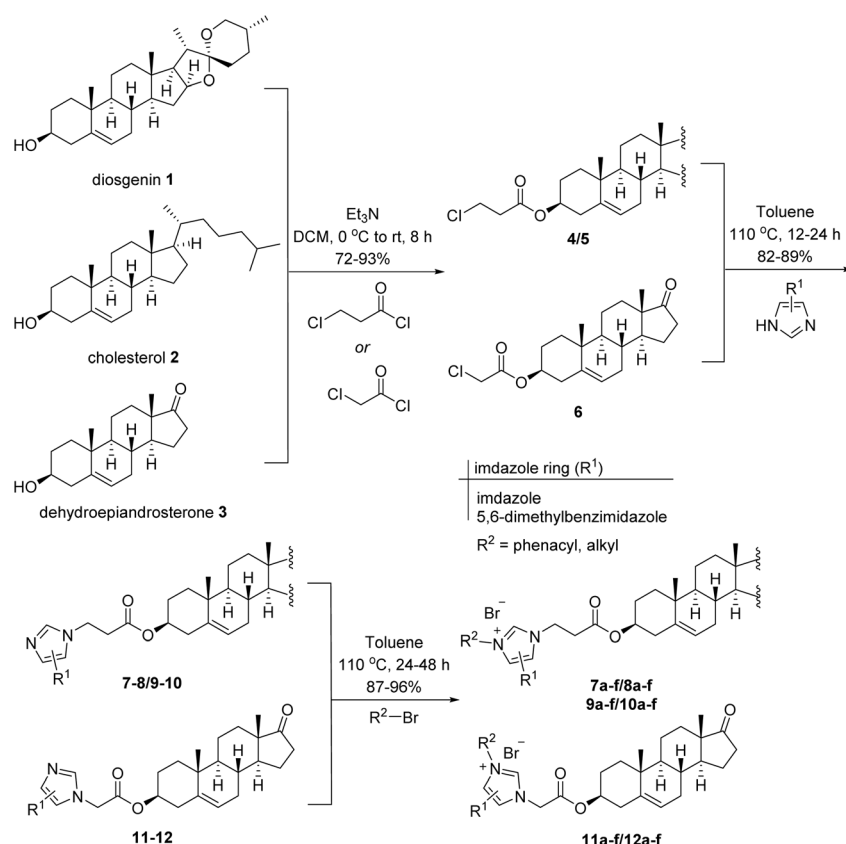
To achieve the synthesis of novel steroid-based imidazolium salt derivatives, we utilized commercially available imidazole

derivatives that were alkylated with esterified 3-hydroxy steroids, which were synthesized from naturally abundant precursors, including diosgenin, cholesterol, and dehydroepiandrosterone. As depicted in Scheme 1, either 3-chloropropionyl chloride or chloroacetyl chloride was employed as the linker to esterify the C3-OH in diosgenin 1, cholesterol 2, and dehydroepiandrosterone 3, respectively, to obtain the chlorinated products 4/5 (72%–75% yields) and 6 (93% yields). Subsequently, the chlorides were converted into six respective 3-substituted steroid-imidazole hybrids (7–8, 9–10, 11–12) by refluxing in toluene with imidazole or 5,6-dimethylbenzimidazole, achieving yields of 82–89%.

Finally, a total of thirty-six imidazolium salt derivatives based on diosgenin, cholesterol, and dehydroepiandrosterone (7a–f/8a–f, 9a–f/10a–f, 11a–f/12a–f) were synthesized by coupling the corresponding imidazolyl-substituted steroidal derivatives with alkyl and phenacyl bromides in refluxing toluene with excellent yields of 87–96%. The structures of these derivatives are presented in Table 1.

Biological evaluation and structure–activity relationship analysis

The cytotoxic potential of all newly synthesized steroid-based imidazole and imidazolium salt derivatives against three human cancer cell lines including breast carcinoma (MDA-MB-231), liver carcinoma (HepG2) and prostate carcinoma (22RV1) were determined using the MTS assay. Cisplatin (DDP), Taxol,



Scheme 1 Synthesis of diosgenin-, cholesterol- and dehydroepiandrosterone-imidazolium salt derivatives.

Table 1 Structures and cytotoxic activities of steroid-based imidazole and imidazolium salt derivatives *in vitro*^b (IC₅₀, ^a μM)

Entry	Compound no.	Steroid	Imidazole ring	R ²	MDA-MB-231	HepG2	22RV1
1	1	—	—	—	>20	>20	>20
2	2	—	—	—	>20	>20	>20
3	3	—	—	—	>20	>20	>20
4	7	Diosgenin	Imidazole	—	>20	>20	>20
5	8	Diosgenin	5,6-Dimethylbenzimidazole	—	>20	>20	>20
6	9	Cholesterol	Imidazole	—	>20	>20	>20
7	10	Cholesterol	5,6-Dimethylbenzimidazole	—	>20	>20	>20
8	11	Dehydroepiandrosterone	Imidazole	—	>20	>20	>20
9	12	Dehydroepiandrosterone	5,6-Dimethylbenzimidazole	—	16.03	16.78	11.10
10	7a	Diosgenin	Imidazole	Phenacyl	4.98	8.22	1.95
11	7b	Diosgenin	Imidazole	4-Bromophenacyl	6.49	8.30	2.38
12	7c	Diosgenin	Imidazole	4-Methylbenzyl	4.17	8.14	1.98
13	7d	Diosgenin	Imidazole	4-Bromobenzyl	5.33	8.22	5.03
14	7e	Diosgenin	Imidazole	2-Cyanobenzyl	5.80	7.16	3.33
15	7f	Diosgenin	Imidazole	1-Naphthylmethyl	5.27	8.83	2.54
16	8a	Diosgenin	5,6-Dimethylbenzimidazole	Phenacyl	6.27	9.86	3.86
17	8b	Diosgenin	5,6-Dimethylbenzimidazole	4-Bromophenacyl	6.63	9.59	4.80
18	8c	Diosgenin	5,6-Dimethylbenzimidazole	4-Methylbenzyl	2.75	2.42	1.20
19	8d	Diosgenin	5,6-Dimethylbenzimidazole	4-Bromobenzyl	5.58	8.37	1.62
20	8e	Diosgenin	5,6-Dimethylbenzimidazole	2-Cyanobenzyl	3.54	3.20	3.03
21	8f	Diosgenin	5,6-Dimethylbenzimidazole	1-Naphthylmethyl	2.18	2.56	2.28
22	9a	Cholesterol	Imidazole	Phenacyl	7.94	18.37	10.32
23	9b	Cholesterol	Imidazole	4-Bromophenacyl	>20	>20	>20
24	9c	Cholesterol	Imidazole	4-Methylbenzyl	3.68	10.44	3.38
25	9d	Cholesterol	Imidazole	4-Bromobenzyl	>20	>20	>20
26	9e	Cholesterol	Imidazole	2-Cyanobenzyl	6.41	8.88	5.58
27	9f	Cholesterol	Imidazole	1-Naphthylmethyl	4.87	13.22	10.37
28	10a	Cholesterol	5,6-Dimethylbenzimidazole	Phenacyl	>20	>20	>20
29	10b	Cholesterol	5,6-Dimethylbenzimidazole	4-Bromophenacyl	>20	>20	>20
30	10c	Cholesterol	5,6-Dimethylbenzimidazole	4-Methylbenzyl	14.96	>20	>20
31	10d	Cholesterol	5,6-Dimethylbenzimidazole	4-Bromobenzyl	>20	>20	>20
32	10e	Cholesterol	5,6-Dimethylbenzimidazole	2-Cyanobenzyl	6.88	11.59	7.58
33	10f	Cholesterol	5,6-Dimethylbenzimidazole	1-Naphthylmethyl	>20	>20	>20
34	11a	Dehydroepiandrosterone	Imidazole	Phenacyl	>20	>20	>20
35	11b	Dehydroepiandrosterone	Imidazole	4-Bromophenacyl	17.33	10.95	>20
36	11c	Dehydroepiandrosterone	Imidazole	4-Methylbenzyl	>20	>20	>20
37	11d	Dehydroepiandrosterone	Imidazole	4-Bromobenzyl	>20	>20	>20
38	11e	Dehydroepiandrosterone	Imidazole	2-Cyanobenzyl	>20	>20	>20
39	11f	Dehydroepiandrosterone	Imidazole	1-Naphthylmethyl	17.46	18.29	8.07
40	12a	Dehydroepiandrosterone	5,6-Dimethylbenzimidazole	Phenacyl	6.81	7.66	4.41
41	12b	Dehydroepiandrosterone	5,6-Dimethylbenzimidazole	4-Bromophenacyl	2.89	2.94	2.71
42	12c	Dehydroepiandrosterone	5,6-Dimethylbenzimidazole	4-Methylbenzyl	2.10	2.71	2.02
43	12d	Dehydroepiandrosterone	5,6-Dimethylbenzimidazole	4-Bromobenzyl	2.89	3.08	1.55
44	12e	Dehydroepiandrosterone	5,6-Dimethylbenzimidazole	2-Cyanobenzyl	7.67	7.58	6.62
45	12f	Dehydroepiandrosterone	5,6-Dimethylbenzimidazole	1-Naphthylmethyl	1.70	2.10	1.07
46	DDP	—	—	—	3.47	4.60	5.10
47	Taxol	—	—	—	<0.008	<0.008	<0.008

^a Cytotoxicity as IC₅₀ for each cell line, is the concentration of compound which reduced by 50% the optical density of treated cells with respect to untreated cells using the MTS assay. ^b Data represent the mean values of three independent determinations.

diosgenin (**1**), cholesterol (**2**), and dehydroepiandrosterone (**3**) were selected as positive controls for efficacy comparison. The results are listed in Table 1.

As shown in Table 1, the single steroidal compounds diosgenin (**1**), cholesterol (**2**), and dehydroepiandrosterone (**3**), which were used as controls, exhibited no activity against all investigated tumor cell lines at a concentration of 20 μM (entries 1–3). For the steroid-based imidazole derivatives (entries 4–9), with the exception of **12**, which features a 5,6-

dimethylbenzimidazole ring linked to the C3-OH of dehydroepiandrosterone via an acetyl group, **12** exhibited relatively weak *in vitro* tumor growth inhibitory activity. The remaining compounds showed no activity against all tested tumor cell lines at a concentration of 20 μM.

Nevertheless, the steroid-based imidazolium salt derivatives (entries 10–45) demonstrated significantly enhanced cytotoxic activities. This can be attributed to the changes in molecular structure, charge distribution and water solubility.¹⁹ For the



three types of steroids, diosgenin-imidazolium salt derivatives (**7a-f/8a-f**) exhibited stable and relatively excellent cytotoxic activities with IC_{50} values of 1.20–9.86 μM *in vitro*. Cholesterol-imidazolium salt derivatives (**9a-f/10a-f**) showed general activities with IC_{50} values of 3.38–18.37 μM or higher than 20 μM . And dehydroepiandrosterone-imidazolium salt derivatives (**11a-f/12a-f**) displayed the optimal activities with IC_{50} values of 1.07–18.29 μM or higher than 20 μM . Among these compounds, eighteen imidazolium salts exhibited higher inhibitory activity against the 22RV1 cell line compared to DDP, with IC_{50} values below 5.10 μM .

For linkers such as acetyl or propionyl, the influence on the cytotoxic activities of steroid-based imidazolium salts was not significant. In the case of the imidazole ring, steroid-based imidazole derivatives (**7a-f/9a-f/11a-f**) with an imidazole ring exhibited moderate inhibitory activity. Among these compounds, diosgenin derivatives demonstrated stable cytotoxic activities with IC_{50} values of 1.95–8.83 μM , while cholesterol and dehydroepiandrosterone derivatives showed weak activities with IC_{50} values of 3.38–18.37 μM or higher than 20 μM . Steroid-based imidazole derivatives (**8a-f/10a-f/12a-f**) with 5,6-dimethylbenzimidazole ring possessed higher inhibitory activity. Among them, diosgenin derivatives (**8c, 8f**) and dehydroepiandrosterone derivatives (**12b-d, 12f**) exhibited significantly higher cytotoxic activities compared to DDP, with IC_{50} values of 1.07–3.08 μM .

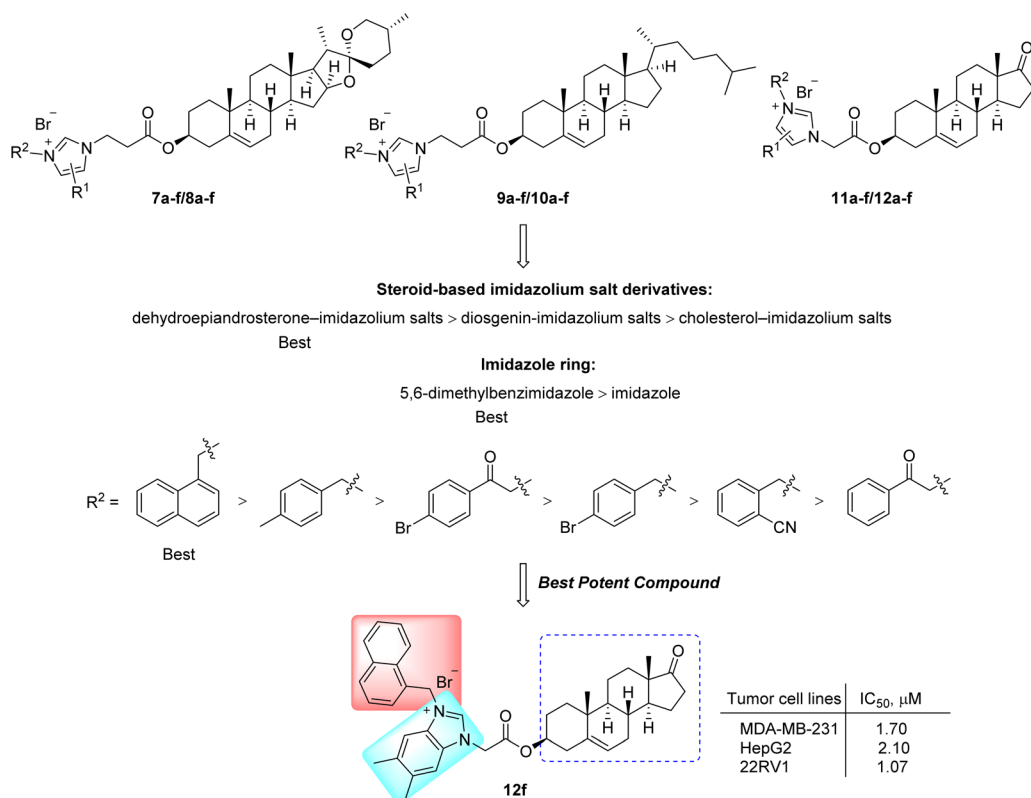
For the substituent at position-3 of the imidazole ring, imidazolium salts bearing phenacyl or 4-bromophenacyl substituent, such as **7a, 7b, 8a, 8b, 9a, 11b** and **12a**, exhibited relatively

weak inhibitory activities against three tumor cell lines. However, compound **12b** demonstrated significantly higher cytotoxic activities compared to DDP with IC_{50} values of 2.71–2.94 μM . Meanwhile, imidazolium salts bearing 4-bromobenzyl or 2-cyanobenzyl substituent, such as **7d, 7e, 8d, 8e, 9e, 12d** and **12e**, exhibited moderate cytotoxic activities ($IC_{50} = 1.55$ –8.88 μM). In contrast, imidazolium salts containing 4-methylbenzyl substituents, such as **8c** and **12c**, as well as 1-naphthylmethyl substituent, such as **8f** and **12f**, demonstrated significantly higher inhibitory activities ($IC_{50} = 1.07$ –2.94 μM) compared to DDP. Notably, dehydroepiandrosterone-imidazolium salt **12f**, bearing a 1-naphthylmethyl substituent at position-3 of 5,6-dimethylbenzimidazole, was identified as the most potent compound, exhibiting IC_{50} values ranging from 1.07 to 2.10 μM against the three investigated human tumor cell lines.

The results indicate that the presence of a substituted 5,6-dimethylbenzimidazole ring and the substitution at the imidazolyl-3-position with either a 1-naphthylmethyl or 4-methylbenzyl group may play a crucial role in enhancing cytotoxic activity. Furthermore, the structure–activity relationship (SAR) results are presented in Scheme 2.

Compound **12f** induces G0/G1 cell cycle arrest and apoptosis in HepG2 cells

To investigate whether the proliferation-inhibitory effect of steroid-based imidazolium salt **12f** was attributable to cell cycle arrest, propidium iodide (PI) staining and flow cytometry analysis were conducted on HepG2 cells treated with various



Scheme 2 Investigation of structure–activity relationships for steroid-based imidazolium salt derivatives.



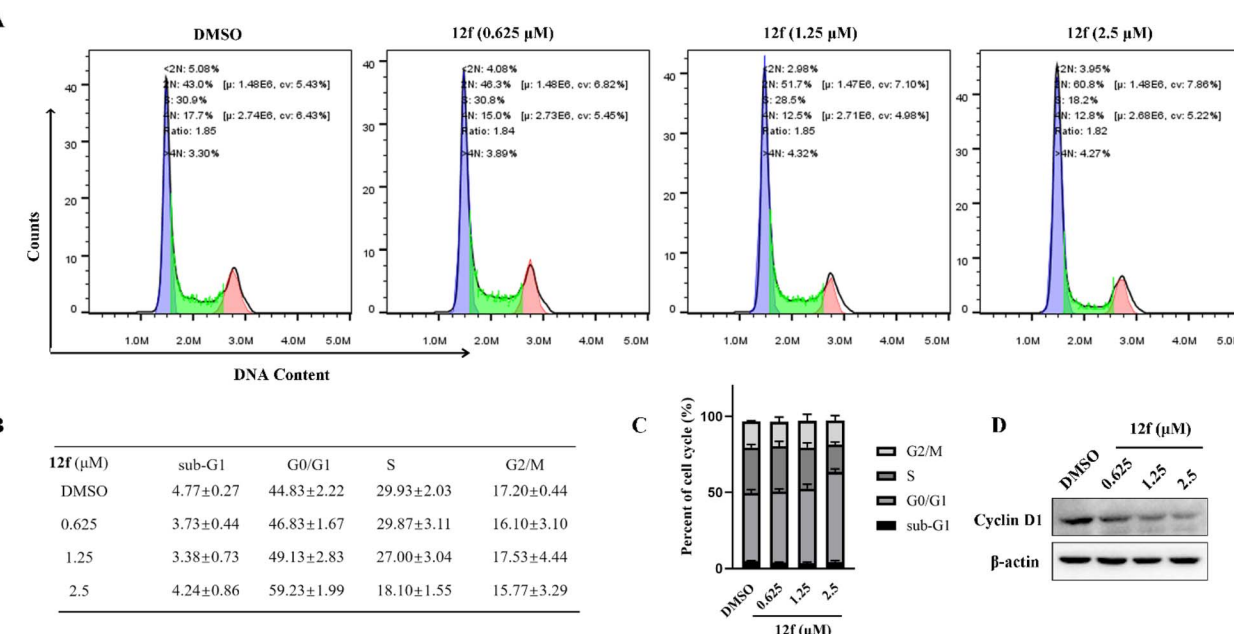


Fig. 2 Compound 12f induces G0/G1 phase arrest in HepG2 cells. (A) Cells were treated with 0.625, 1.25 and 2.5 μM of compound 12f for 24 hours. The cell cycle was analyzed using PI staining in combination with flow cytometry. (B) The percentages of cells in different phases were quantified. At least three independent experiments were performed, and the data from a representative experiment are shown. (C) The percentages of cells in different phases were quantified. (D) The protein level of Cyclin D1 was detected with western blot analysis with β-actin was used as a loading control.

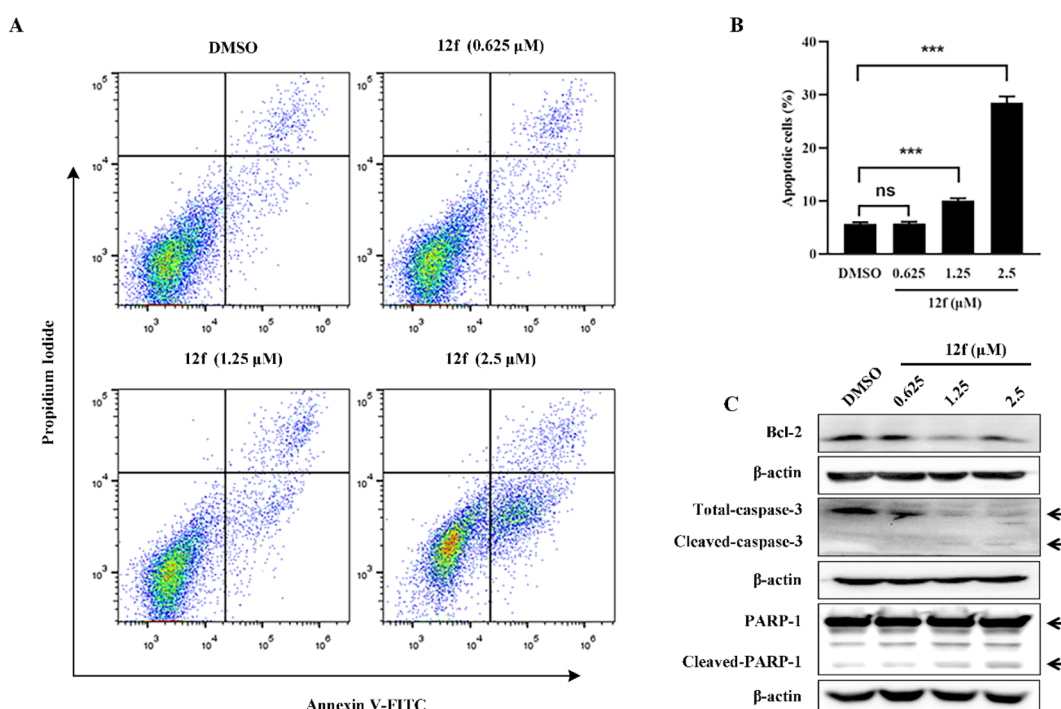
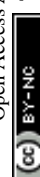


Fig. 3 Compound 12f caused significant apoptosis of HepG2 cells. (A) Cells were treated with 0.625, 1.25 and 2.5 μM compound 12f for 48 hours. Cell apoptosis was determined by Annexin V-FITC/PI double-staining assay. (B) The quantification of cell apoptosis. (C) The protein level of apoptosis related proteins of Bcl-2, total and cleaved-caspase 3 and PARP-1 were detected with western blot analysis with β-actin was used as a loading control. The asterisk (*) represents a statistically significant difference when compared to the DMSO group (*P < 0.05, **P < 0.01, ***P < 0.001), while "ns" indicates not significant (P > 0.05). Error bars represent the standard deviation (SD) of the mean.



concentrations of **12f** (0.625, 1.25, and 2.5 μ M). As illustrated in Fig. 2, imidazolium salt **12f** induced G0/G1 cell cycle arrest in a dose-dependent manner. Specifically, the proportion of cells in the G0/G1 phase increased to 49.13% and 59.23% for those treated with 1.25 μ M and 2.5 μ M of **12f**, respectively, compared to 44.83% in the control group. Conversely, the proportions of cells in the S phase and G2/M phase were decreased to 18.10% and 15.77%, respectively, in the group treated with 2.5 μ M imidazolium salt **12f**, compared to 29.93% and 17.20% in the control group. Meanwhile, the proportion of sub-G1 phase cells did not show a significant change. Of note, the protein level of Cyclin D1, a key regulator of inducing the transition from G0/G1 to S phase, was dominantly downregulated.

The imidazolium salt **12f**-induced cell apoptosis was assessed using Annexin V-FITC/PI double-labeled flow cytometry. As illustrated in Fig. 3, after treating HepG2 cells with **12f** at concentrations of 1.25 μ M and 2.5 μ M for 48 hours, the apoptosis rates significantly increased to 10.08% and 28.53%, respectively. However, no significant difference was observed at 0.625 μ M. Furthermore, the anti-apoptotic protein Bcl-2 was attenuated, with induction of the cleavage of caspase 3 and PARP-1 detected. These results indicate that the imidazolium salt **12f** inhibits cell proliferation by inducing G0/G1 cell cycle arrest and apoptosis in HepG2 cells.

Conclusion

In summary, three series of novel steroid-based imidazolium salt derivatives were successfully synthesized and exhibited significant antitumor activities *in vitro*. The results indicated that the dehydroepiandrosterone-imidazolium salt derivatives with 5,6-dimethylbenzimidazole ring exhibited higher cytotoxic activities than diosgenin-imidazolium salts and cholesterol-imidazolium salts. Furthermore, the substitution at the imidazolyl-3-position with a 1-naphthylmethyl or 4-methylbenzyl group may play a crucial role in enhancing cytotoxic activity. The dehydroepiandrosterone-imidazolium salt derivatives **12b-d** and **12f**, with 5,6-dimethylbenzimidazole ring and a 4-bromophenacyl, 4-methylbenzyl, 4-bromobenzyl or 1-naphthylmethyl group at imidazolyl-3-position, exhibited higher inhibitory activity compared to DDP. Compound **12f** can induce the G0/G1 phase cell cycle arrest and apoptosis in HepG2 cells. The steroid-based imidazolium salt derivatives **8c**, **8f**, **12b-d** and **12f** demonstrated potential as a new starting point for the discovery of promising lead compounds, which may be further leveraged in the development of innovative anticancer agents.

Experimental section

General procedures

Melting points were determined using an XT-4 melting point apparatus and were reported without correction. Proton nuclear magnetic resonance (1 H-NMR) spectra were recorded on a Bruker Avance 400 spectrometer operating at 400 MHz. Carbon-13 nuclear magnetic resonance (13 C-NMR) spectra were recorded on the same instrument operating at 100 MHz. Chemical shifts are expressed as δ values in parts per million

(ppm) with tetramethylsilane (TMS) used as the reference standard for all NMR measurements. High-resolution mass spectra were obtained using an AB Sciex QSTAR Pulsar mass spectrometer. The silica gel (200–300 mesh) used for column chromatography and silica GF254 used for TLC were supplied by Qingdao Marine Chemical Company (China). All air- and moisture-sensitive reactions were carried out under an argon atmosphere. The starting materials and reagents employed in the reactions were purchased from Adamas, Acros and Sigma-Aldrich and were used without further purification unless otherwise specified.

Synthesis of compounds 4/5/6. Diosgenin **1** (4.2 g, 10.0 mmol), cholesterol **2** (3.9 g, 10.0 mmol), and dehydroepiandrosterone **3** (2.9 g, 10.0 mmol) were dissolved separately in dichloromethane (30.0 mL). Subsequently, 3-chloropropionyl chloride (1.1 mL, 12.0 mmol) and triethylamine (2.8 mL, 20.0 mmol) were added to the solutions of **1** and **2**, respectively, while 2-chloroacetyl chloride (0.9 mL, 12.0 mmol) and triethylamine (2.8 mL, 20.0 mmol) were introduced into the solution of **3** at 0 °C. The resulting mixture was stirred at room temperature for 8 hours. The reaction progress was monitored using TLC. A small amount of water was added and the mixture was stirred for 15 minutes. The aqueous phase was washed with CH_2Cl_2 (3 \times 20 mL). The combined organic phase was dried over Na_2SO_4 and concentrated. The residue was purified using column chromatography on silica gel (petroleum ether : EtOAc = 20 : 1) to yield products **4** (3.6 g, 72%), **5** (3.8 g, 79%), and **6** (3.4 g, 93%), respectively, all obtained as white solids. See the SI file for characterization data.

Synthesis of compounds 7-8/9-10/11-12. A mixture of the previously obtained chlorinated product (3.0 mmol) and imidazole or 5,6-dimethylbenzimidazole (15.0 mmol) was refluxed in toluene (20.0 mL) for 12–24 hours under continuous stirring, with reaction progress monitored by TLC. After cooling to room temperature, the solvent was concentrated, and the residue was diluted with EtOAc (20.0 mL). The organic layer was washed with water (20.0 mL) and brine (20.0 mL), dried over anhydrous Na_2SO_4 and concentrated. The residue was purified by column chromatography (silica gel, EtOAc : MeOH : Et_3N = 100 : 1 : 0.1) to afford **7-8/9-10/11-12** in 82–89% yield as white powder. See the SI file for characterization data.

Synthesis of compounds 7a-f/8a-f/9a-f/10a-f/11a-f/12a-f. A mixture of imidazole compounds **7-8/9-10/11-12** (0.2 mmol) and phenacyl bromide or alkyl bromides (0.4 mmol) was refluxed in toluene (10.0 mL) for 24–48 hours under continuous stirring. An insoluble substance was formed. Upon completion of the reaction, as confirmed by TLC, the precipitate was filtered through a short Celite pad and rinsed with ethyl acetate (3 \times 10.0 mL), followed by drying to yield imidazolium salts **7a-f/8a-f/9a-f/10a-f/11a-f/12a-f** in 87–96% yields. See the SI file for characterization data.

Cytotoxicity assay. The assay was conducted using three types of cell line: MDA-MB-231, HepG2, and 22RV1. The cells were cultured at 37 °C in a humidified atmosphere containing 5% CO_2 in RPMI 1640 medium supplemented with 10% fetal bovine serum and seeded in replicate 96-well plates. Following cell seeding, the compounds were added. After 48 hours of



exposure, cell viability was assessed using the [3-(4,5-dimethylthiazol-2-yl)-5-(3-carboxymethoxyphenyl)-2-(4-sulfo-phenyl)-2*H*-tetrazolium] (MTS) cytotoxicity assay by measuring absorbance at 490 nm with a microplate spectrophotometer. All experiments were performed in triplicate.

Cell cycle analysis. To analyze the DNA content by flow cytometry, cells were harvested and washed twice with phosphate-buffered saline (PBS). Cells were fixed with 70% ethanol overnight. Following fixation, the cells were rinsed with PBS and subsequently stained with a solution containing 50 µg per mL propidium iodide (PI) and 50 µg per mL RNase A for 30 minutes at room temperature. Fluorescence intensity was assessed using a FACSCalibur flow cytometer (BD Biosciences, San Jose, CA, USA). The percentages of cells in different phases of the cell cycle were determined using FlowJo Version 7.6.1 software.

Cell apoptosis analysis. Cell apoptosis was evaluated using the Annexin V-FITC/PI Apoptosis Kit (BD Biosciences, Franklin Lakes, NJ) in accordance with the manufacturer's instructions. Cells were seeded in 6-well plates at a density of 3.0×10^5 cells per well. Following 48 hours of treatment with the compound at the specified concentrations, the cells were harvested, washed twice with cold phosphate-buffered saline (PBS), and resuspended in binding buffer containing Annexin V-FITC and propidium iodide (PI). After incubation for 15 minutes at room temperature in the dark, fluorescence intensity was analyzed using a FACSCalibur flow cytometer (BD Biosciences, Franklin Lakes, NJ).

Western blot analysis. The western blot analysis was performed as previously.¹⁶ The antibodies against Bcl-2, caspase-3, PARP-1 and β-actin were obtained from Proteintech, while the Cyclin D1 antibody was bought from Santa Cruz.

Author contributions

G. G. D. and L. M. K. conceived the project. T. T. L., L. J. F., and Y. L. L. performed the chemical experiments. Y. Y. P., A. R. L., and M. Y. H. performed the cell activity experiments. T. T. L., Y. P., and Z. H. Z. analysed and interpreted the experimental data. G. G. D. and L. M. K. drafted the paper and supervised the project. All the authors discussed the results and contributed to the preparation of the final manuscript.

Conflicts of interest

There are no conflicts of interest to declare.

Data availability

All data supporting the results of this study are available within the article and its SI files. Supplementary information is available. See DOI: <https://doi.org/10.1039/d5ra05514h>.

Acknowledgements

This work was supported by Yun-nan Fundamental Research Projects (202301AU070198 and 202501AT070181), Xingdian

Talents Support Program for G. G. D. and L. M. K., The 2025 Central Government Project for Supporting the Reform and Development of Local Universities-Special Project for the Construction of an Interdisciplinary "Comprehensive Health" Medical-Education Integration Innovation Platform.

References

- J. M. Kocarnik, K. Compton, F. Dean, W. Fu, B. Gaw, J. Harvey, H. Henrikson, D. Lu, A. Pennini, R. Xu and F. Lisa, *J. Clin. Oncol.*, 2021, **39**, 10577.
- F. Bray, M. Laversanne, H. Sung, J. Ferlay, R. L. Siegel, I. Soerjomataram and A. Jemal, *Ca-Cancer J. Clin.*, 2024, **74**, 229.
- B. Chopra and A. K. Dhingra, *Phytother. Res.*, 2021, **35**, 4660.
- D. J. Newman and G. M. Cragg, *J. Nat. Prod.*, 2020, **83**, 770.
- (a) F. Wang, L. Liang, M. Yu, W. Wang, I. H. Badar, Y. Bao, K. Zhu, Y. Li, S. Shafi, D. Li, Y. Diao, T. Efferth, Z. Xue and X. Hua, *Phytomedicine*, 2024, **128**, 155432; (b) D. F. Mendoza Lara, M. E. Hernández-Caballero, J. L. Terán, J. S. Ramírez and A. Carrasco-Carballo, *ACS Omega*, 2025, **10**, 7493.
- (a) M. Li, H. Luo, Z. Huang, J. Qi and B. Yu, *Molecules*, 2022, **28**, 295; (b) W. Yin, H. Xue, Y. Zhang, R. Li, M. Liu, H. Yue, D. Ge and N. Liu, *Eur. J. Pharmacol.*, 2025, **998**, 177512.
- X.-J. Qin, D.-J. Sun, W. Ni, C.-X. Chen, Y. Hua, L. He and H.-Y. Liu, *Steroids*, 2012, **77**, 1242.
- N. V. Ivanchina, A. A. Kicha, T. V. Malyarenko, S. D. Ermolaeva, E. A. Yurchenko, E. A. Pislyagin, M. C. Van and P. S. Dmitrenok, *Nat. Prod. Res.*, 2019, **33**, 2623.
- L. Fernández-Cabezón, B. Galán and J. L. García, *Front. Microbiol.*, 2018, **9**, 958.
- (a) S. N. Riduan and Y. Zhang, *Chem. Soc. Rev.*, 2013, **42**, 9055; (b) J. Lee, J.-G. Kim, H. Lee, T. H. Lee, K.-Y. Kim and H. Kim, *Pharmaceutics*, 2021, **13**, 312; (c) M. Malinowska, D. Sawicka, K. Niemirowicz-Laskowska, P. Wielgat, H. Car, T. Hauschild and A. Hryniiewicka, *Int. J. Mol. Sci.*, 2021, **22**, 12180; (d) F. G. Baldissera, T. Fazolo, M. B. da Silva, P. C. de Santana Filho, V. D. da Silva, D. M. Rivillo Perez, J. S. Klitzke, E. G. de Oliveira Soares, L. C. Rodrigues Júnior, A. Peres, E. Dallegrave, K. C. Navegantes-Lima, M. C. Monteiro, H. S. Schrekker and P. R. Torres Romão, *Front. Immunol.*, 2023, **13**, 1096312.
- (a) M. A. DeBord, M. R. Southerland, P. O. Wagers, K. M. Tiemann, N. K. Robishaw, K. T. Whiddon, M. C. Konopka, C. A. Tessier, L. P. Shriver, S. Paruchuri, D. A. Hunstad, M. J. Panzner and W. J. Youngs, *Bioorg. Med. Chem. Lett.*, 2017, **27**, 764; (b) M. A. DeBord, P. O. Wagers, S. R. Crabtree, C. A. Tessier, M. J. Panzner and W. J. Youngs, *Bioorg. Med. Chem. Lett.*, 2017, **27**, 196; (c) H. S. Al-Buthabhab, Y. Yu, A. Sobolev, H. Al-Salami and M. V. Baker, *J. Inclusion Phenom. Macrocyclic Chem.*, 2021, **101**, 227.
- (a) X.-Q. Wang, L.-X. Liu, Y. Li, C.-J. Sun, W. Chen, L. Li, H.-B. Zhang and X.-D. Yang, *Eur. J. Med. Chem.*, 2013, **62**, 111; (b) Y. Zhou, K. Duan, L. Zhu, Z. Liu, C. Zhang,



L. Yang, M. Li, H. Zhang and X. Yang, *Bioorg. Med. Chem. Lett.*, 2016, **26**, 460.

13 L.-X. Liu, X.-Q. Wang, J.-M. Yan, Y. Li, C.-J. Sun, W. Chen, B. Zhou, H.-B. Zhang and X.-D. Yang, *Eur. J. Med. Chem.*, 2013, **66**, 423.

14 M. Yin, Y. Fang, X. Sun, M. Xue, C. Zhang, Z. Zhu, Y. Meng, L. Kong, Y. Y. Myint, Y. Li, J. Zhao and X. Yang, *Front. Chem.*, 2023, **11**, 1191498.

15 (a) G. Deng, B. Zhou, J. Wang, Z. Chen, L. Gong, Y. Gong, D. Wu, Y. Li, H. Zhang and X. Yang, *Eur. J. Med. Chem.*, 2019, **168**, 232; (b) X.-L. Xu, J. Wang, C.-L. Yu, W. Chen, Y.-C. Li, Y. Li, H.-B. Zhang and X.-D. Yang, *Bioorg. Med. Chem. Lett.*, 2014, **24**, 4926; (c) X.-L. Xu, C.-L. Yu, W. Chen, Y.-C. Li, L.-J. Yang, Y. Li, H.-B. Zhang and X.-D. Yang, *Org. Biomol. Chem.*, 2015, **13**, 1550; (d) B. Zhou, Z.-F. Liu, G.-G. Deng, W. Chen, M.-Y. Li, L.-J. Yang, Y. Li, X.-D. Yang and H.-B. Zhang, *Org. Biomol. Chem.*, 2016, **14**, 9423; (e) C.-B. Zhang, Y. Liu, Z.-F. Liu, S.-Z. Duan, M.-Y. Li, W. Chen, Y. Li, H.-B. Zhang and X.-D. Yang, *Bioorg. Med. Chem. Lett.*, 2017, **27**, 1808; (f) M. Huang, S. Duan, X. Ma, B. Cai, D. Wu, Y. Li, L. Li, H. Zhang and X. Yang, *Med. Chem. Commun.*, 2019, **10**, 1027.

16 H. Zhou, C. Yu, L. Kong, X. Xu, J. Yan, Y. Li, T. An, L. Gong, Y. Gong, H. Zhu, H. Zhang, X. Yang and Y. Li, *Oncogene*, 2019, **38**, 3371.

17 (a) D. C. Blakemore, L. Castro, I. Churcher, D. C. Rees, A. W. Thomas, D. M. Wilson and A. Wood, *Nat. Chem.*, 2018, **10**, 383; (b) W. P. Walters, J. Green, J. R. Weiss and M. A. Murcko, *J. Med. Chem.*, 2011, **54**, 6405.

18 T. Cernak, K. D. Dykstra, S. Tyagarajan, P. Vachal and S. W. Krska, *Chem. Soc. Rev.*, 2016, **45**, 546.

19 J. Ranke, S. Stolte, R. Störmann, J. Arning and B. Jastorff, *Chem. Rev.*, 2007, **107**, 2183.

